Journal of Southeast University (English Edition) Vol. 40, No. 2, pp. 155 - 164 June 2024 ISSN 1003—7985

Multihazard risk assessment of sea-crossing suspension bridges based on an improved Bayesian network method

Liu Chengyin[1,2] Ren Lichen[1,2] Jiang Zhaoshuo[3] Fang Qiyang[1,2]

([1]School of Civil and Environmental Engineering, Harbin Institute of Technology(Shenzhen), Shenzhen 518055, China)

([2]Guangdong Provincial Key Laboratory of Intelligent and Resilient Structures for Civil Engineering, Harbin Institute of Technology(Shenzhen), Shenzhen 518055, China)

([3]School of Engineering, San Francisco State University, San Francisco 94132, USA)

Abstract: To assess the combined risks of long-span suspension bridges under continuous wind loads and occasional earthquakes, a risk assessment framework for cross-sea suspension bridges based on improved Bayesian networks was proposed by combining the quantitative analysis of the structural damage probability and the qualitative assessment of the damage consequences during bridge operation. First, the damage degree of each component was obtained according to the characteristics of the suspension bridge and the results of wind and earthquake analyses. Then, the failure probability of the bridge structure was calculated using the theory of structural reliability. Finally, the risk assessment model of the suspension bridge based on improved Bayesian networks was proposed to evaluate the risk during bridge operation. The results show that considering the varying impacts of different bridge components, the bridge damage level can be categorized into four degrees based on its disaster resilience. Taking the Lingdingyang Bridge as an example, the maximum risk level under multihazard risks is level 3 according to the proposed method, which requires traffic restrictions and maintenance. Therefore, this method can guide the emergency management strategy of sea-crossing bridges in response to multihazard risks.

Key words: sea-crossing suspension bridge; risk assessment; Bayesian network; damage index; structural reliability

DOI: 10.3969/j.issn.1003-7985.2024.02.006

Risks to bridges during their operational period include accidents caused by winds, earthquakes, fires, hydraulic events, collisions, and fatigue. In this respect, risk analysis generally aims to evaluate the possibility of risks and develop corresponding countermeasures[1]. As suspension bridges are often used as long-span bridges, the demand for suspension bridges and their maintenance in China are increasing[2]. For suspension bridges, 58.4% of related accidents are caused by wind disasters[3], and earthquakes may result in catastrophic consequences. Therefore, they are chosen as typical risks. In this regard, Lu et al.[4] developed a procedure to assess the seismic performance of the overall system for long-span suspension bridges. Meanwhile, Hu et al.[5] used a health monitoring system for the wind resistance evaluation of long-span suspension bridges. Currently, there are two challenges in evaluating suspension bridges. First, the structural compositions of suspension bridges are both diverse and complex, requiring systematic assessment. Second, this area lacks an assessment model that integrates both qualitative and quantitative approaches.

Given the complex nature of sea-crossing suspension bridges, which consist of numerous components, Bayesian networks[6-7] have gained widespread use in risk assessment because of their ability to depict the relationships between component risk nodes. Meanwhile, to address the lack of quantitative assessments, the response surface method[8] and the equivalent normalizing method (JC method)[9] are introduced. The response surface method, in conjunction with the JC method, enables rapid and accurate calculation of bridge damage probability, considering uncertainties associated with a bridge's structural material. Because specific risk acceptance criteria for suspension bridges are lacking, this study combines quantitative risk probability with qualitative risk assessment based on the "as low as reasonably practicable" principle to express the evaluation indices of earthquake and wind damage. The damage consequences are categorized into minor, medium, severe, and complete damage based on the acceptable levels for sea-crossing bridges. Consequently, suspension bridges are classified into four risk levels, ranging from levels 1 to 4.

This study proposes a multihazard risk assessment

Received 2024-01-18, **Revised** 2024-03-28.

Biographies: Liu Chengyin (1978—), male, doctor, professor; Jiang Zhaoshuo (corresponding author), male, doctor, associate professor, zsjiang@sfsu.edu.

Foundation items: The National Key Research and Development Program of China (No. 2022YFB2602105), the National Natural Science Foundation of China (No. 52378295), Guangdong Province Natural Science Foundation (No. 2024A1515010296), Guangdong Provincial Key Laboratory of Intelligent and Resilient Structures for Civil Engineering (No. 2023B1212010004), Shenzhen Science and Technology Program (No. KQTD20210811090112003).

Citation: Liu Chengyin, Ren Lichen, Jiang Zhaoshuo, et al. Multihazard risk assessment of sea-crossing suspension bridges based on an improved Bayesian network method[J]. Journal of Southeast University (English Edition), 2024, 40(2): 155 - 164. DOI: 10.3969/j.issn.1003-7985.2024.02.006.

framework based on improved Bayesian networks to evaluate the risks of sea-crossing suspension bridges under wind disasters and earthquakes. Leveraging Bayesian networks, the framework effectively considers both types of risks associated with suspension bridges.

1 Risk Assessment Methodology Based on an Improved Bayesian Network

As complex structural systems, sea-crossing suspension bridges incorporate various structural components. To assess the overall system risk probability, this paper employed an improved Bayesian network that integrates the results of component risk probabilities.

1.1 Suspension bridge reliability analysis

The limit state equation for reliability analysis of suspension bridge structures can be defined as follows:

$$Z = R_i - S_{i\max} \tag{1}$$

where Z represents the limit state function of the i-th element; R_i represents the capacity of the i-th element; $S_{i\max}$ represents the maximum structural response of the i-th element.

Because of the nonlinearity in large structures, the response surface method is employed to approximate the function of complex structures using a simple and explicit formula as following:

$$Z = g(X_1, X_2, \ldots, X_n) = a + \sum_{i=1}^{n} b_i X_i + \sum_{i \neq j}^{n} \sum c_{ij} X_i X_j \tag{2}$$

where $X_i (i = 1, 2, \ldots, n)$ are basic random design variables; a, b_i, c_{ij} are the coefficients to be determined.

Using the JC method, nonnormal basic random variables are normalized into equivalent normal random variables. This transformation process must satisfy the constraint condition, wherein the probability distribution function and probability density function values of the original nonnormal variables should be equal to the transformed normal variables at checking points. Given this constraint condition, the following equations can be derived:

$$\sigma_{Y_i} = \frac{\varphi[\varphi^{-1} F_{X_i}(X_i^*)]}{f_{X_i}(X_i^*)} \tag{3}$$

$$u_{Y_i} = X_i^* - \varphi^{-1} F_{X_i}(X_i^*) \sigma_{Y_i} \tag{4}$$

where φ is the standard normal distribution function; φ^{-1} is the inverse function of the standard normal distribution function; u_{Y_i} and σ_{Y_i} are the mean and standard deviation of the normal distribution random scalar Y_i; $F_{X_i}(X_i^*)$ and $f_{X_i}(X_i^*)$ are the probability distribution function and probability density function values of the random variable at the checking point X_i^*, respectively.

To solve the reliability index of a bridge structure, the improved first-order second-moment method is employed[9]. Specifically, the reliability index can be obtained by simultaneously solving the following three equations:

$$\cos\theta_{Y_i} = \frac{-\left.\frac{g}{Y_i}\right/ (P^* \sigma_{Y_i})}{\left[\sum_{i=1}^{n} \left(-\left.\frac{g}{Y_i}\right/ (P^* \sigma_{Y_i})\right)^2\right]^{1/2}} \tag{5}$$

$$y_i^* = u_{Y_i} + \beta \sigma_{Y_i} \cos\theta_{Y_i} \qquad i = 1, 2, \ldots, n \tag{6}$$

$$g_Y(Y_1^*, Y_2^*, \ldots, Y_n^*) = 0 \tag{7}$$

where P^* represents design points on Ω_Y spatial limit state surface and θ_{Y_i} is the limit state surface at the checking point P^*.

1.2 Summary of suspension bridge risk assessment Bayesian network

The Bayesian network can effectively combine the quantitative analysis of structural damage probability with the qualitative analysis of damage consequences, making it suitable for risk assessment in engineering projects. It allows the analysis of failure probabilities influenced by multiple uncertain factors and facilitates reasoning about project risk probabilities. To visually illustrate this process, Figs. 1 and 2 depict the upper and lower structures of the Bayesian network for the reliability of suspension bridge systems.

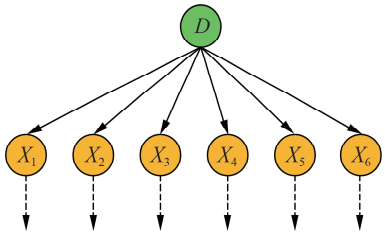

Fig. 1 Superstructure

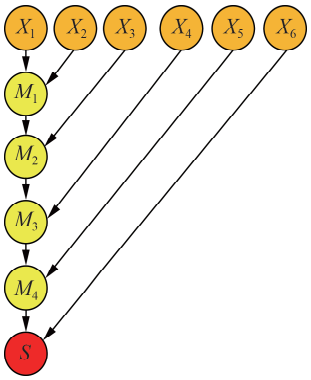

Fig. 2 Substructure

In the upper structure of the Bayesian network, the root node D represents dangerous events on n components,

while X represents failure events at each component level. The downstream portion of the Bayesian network begins with component events and deals with the estimation of failure events at a system level. Because of limitations in the conditional probability table's size, this study did not employ a single system-level node as a child node for all component nodes as it would be computationally impractical. Assuming a binary state for failure events, a system with n components would result in a conditional probability table with 2^{n+1} elements. Each of these component subsets corresponds to a series subsystem. To reduce the number of parent nodes and the size of the conditional probability table for each subsystem, a set of intermediate nodes can be defined. To simplify the calculation of the Bayesian network structure, M modes, as shown in Fig. 2, are applied, resulting in each child node having only two parent nodes. The formula for calculating the probability of occurrence of a child node with two parent nodes is shown as

$$P(S=1) = \sum_{X_1, X_2} P(S=1 \mid X_1, X_2) P(X_1) P(X_2) \quad (8)$$

where $P(S=1)$ represents the probability of occurrence of child nodes; $P(X_1)$ and $P(X_2)$ represent the occurrence probabilities of parent nodes; $P(S=1 \mid X_1, X_2)$ represents the probability of occurrence of P under the condition of occurrence of X_1 or X_2.

When bridge components can enter multiple damage states, each component's damage state must be considered as a potential contributor to one of the failure modes of the system. For instance, a bridge tower in a slightly damaged state represents a different failure mode compared with a bridge tower in a collapsed state. Fig. 3 illustrates such a model, wherein an intermediate component node with binary output is inserted to decompose the state of the initial component node. Assuming that each of the six components has two states and each X_i node generates two child nodes X_{i1} and X_{i2} enables treating the damage status of each component as a separate factor for different system failure modes.

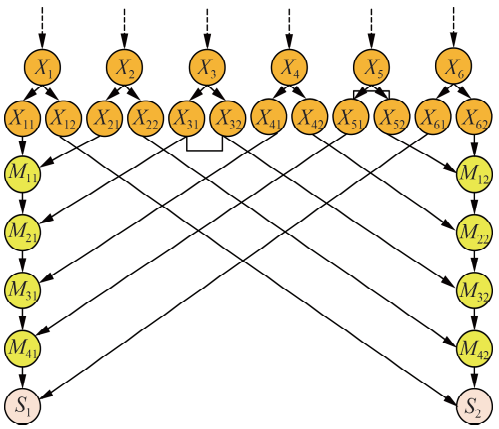

Fig. 3 Bayesian network model with multiple failure modes

The above assumption also facilitates coordinating the formulas of various intermediate nodes, with all intermediate nodes being describable using binary states. Although the example presented in this paper assumes that each type of component damage state results in the same system failure mode, different component damage states always happen and can be combined in practical situations.

The abovementioned improved Bayesian network was implemented using the Bayesian network toolbox in MATLAB[10]. The network can be generated using simple algorithms, and the basic network can be easily expanded to automatically generate more complex Bayesian networks for various needs.

1.3 Suspension bridge multihazard risk assessment framework based on improved Bayesian networks

The proposed framework for multihazard risk assessment of suspension bridges, based on improved Bayesian networks, is depicted in Fig. 4. The first step is to determine the main loads, which are wind and earthquake in this research. The next step is to identify the key components of suspension bridges based on finite element analysis(FEA). Then, after obtaining the damage index in the third step, the following step involves calculating the damage probability of the key components using the JC method while fitting the limit state equation of the structure using the response surface method. Finally, an improved Bayesian network structure is established and applied for the risk assessment of suspension bridges.

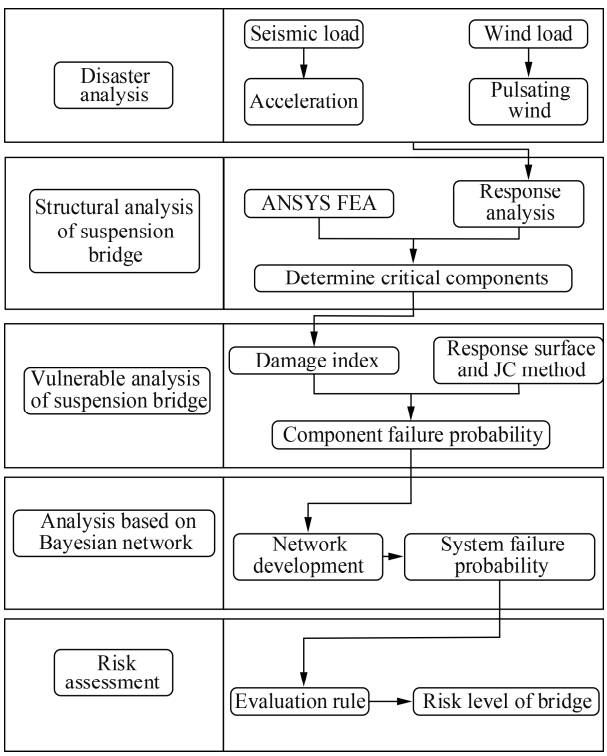

Fig. 4 Risk assessment framework of suspension bridge based on improved Bayesian network

2 Case Study of a Suspension Bridge System

2.1 Background of Lingdingyang Bridge

Lingdingyang Bridge (LDYB), depicted in Fig. 5, is a sea-crossing suspension bridge with a span of 1 666 m. Its tower is a portal structure measuring 270 m high. Its suspension hangers are typically reinforced suspension hangers and ordinary nonreinforced hangers. Its structural response must be obtained using the finite element method (FEM). Therefore, a FEM of LDYB was established using the ANSYS finite element software. The structural layout of LDYB is shown in Fig. 6.

Fig. 5 Schematic diagram of the LDYB

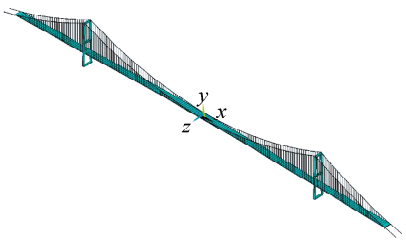

Fig. 6 Finite element three-dimensional view of LDYB

The bridge structural model consisted of five parts: the tower, pier, main cable, hanger, and main girder. After establishing the model, the dynamic characteristics of the structure were analyzed. The first six natural frequencies of the model were compared with those from past studies[11-12], which demonstrated the accuracy of the developed model of this research.

2.2 Disaster load at the bridge location

2.2.1 Wind load

The impact of wind load on the bridge considers the effects of wind-induced buffeting. Wind can generally be regarded as the combination of mean wind and pulsating wind[13]. The mean wind has a fixed direction and value, which can be represented by a static wind direction and value. The average effect of pulsating wind is treated as a static load acting on the structure. In this study, the wind speed time history of fluctuating wind was simulated using the linear filtering method of an autoregressive model[14], whereas the wind speed spectrum was based on the Davenport spectrum[15]. For LDYB, the sea wind parameters could be determined on the basis of meteorological observations and wind parameter studies conducted at the location of the Shenzhen-Zhongshan Link[16].

2.2.2 Seismic load

According to a study on regional seismicity and seismological structures[17], the study site presented three probability levels (i. e., 63%, 5%, and 2%) exceeding the 100-year seismic design reference period. The dynamic design parameters included the peak acceleration of the ground surface and ground motion design parameters. To calculate the design horizontal motion acceleration response spectrum and seismic influence coefficient of the bridge, previous methods[17] were utilized. Subsequently, seismic waves could be synthesized using the trigonometric series method[18] based on the seismic characteristics.

2.3 Selection of key components and division of damage indicators

2.3.1 Bridge response analysis and key components

In practice, the most common approach for failure probability calculation is monitoring critical locations of bridges. However, as the structure of LDYB is symmetrical horizontally, only critical components (see Fig. 7) on one side of the bridge were selected for failure probability calculation. The determination of the key components was based on the analysis result of the FEM under self-weight, wind loads with a 100-year recurrence period, and earthquake load with a 2% exceedance probability. The suspension bridge could be divided into five key components: hangers, main girders, main cables, towers, and piers. After applying designated load operating conditions, the critical positions were identified based on where the maximum load effect was observed for each

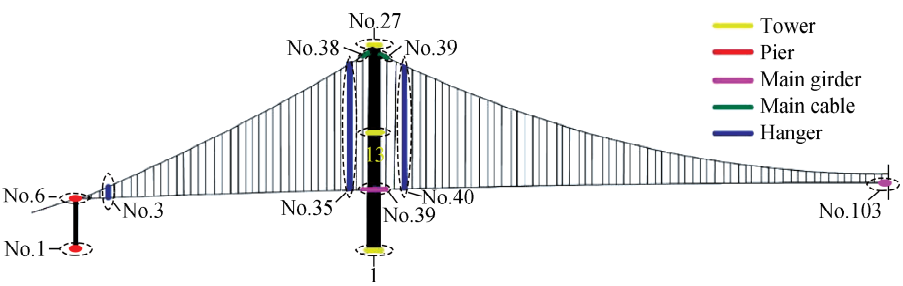

Fig. 7 Key components of LDYB

component: Nos. 3, 35, and 40 for the hangers, Nos. 38 and 39 for the cables, No. 103 for the girder, Nos. 1, 13, and 27 for the tower, and Nos. 1 and 6 for the piers. The numbers in Fig. 7 represent the number of elements in the finite element software.

2.3.2 Suspension bridge structure damage index

Ref. [19] qualitatively evaluated the risks associated with the wind resistance performance of bridge structures. Accordingly, towers, piers, and main cables were considered as the primary load-bearing components of suspension bridges. Their failure was considered complete damage to the entire structure. Additionally, complete damage to the main girder would lead to severe damage to the entire bridge. Meanwhile, individual damage to the suspension hangers did not result in significant harm to suspension bridges, whereas complete damage to each hanger corresponded to moderate damage. Complete damage to the bridge tower corresponded to the catastrophic failure of bridges.

Drawing on previous studies regarding the seismic damage limitations of tall piers and chimneys[20-21], this study utilized the curvature index to classify the damage grades of tower sections. For the main girder, to determine the extent of damage, a quantitative approach was employed, dividing the damage level based on the stress experienced by the main girder. In the case of LDYB, the main girder was a Q345 steel box girder[22]. The damage index of the main girder was defined considering its design values of strength, yield strength, and ultimate failure strength. Because of the high redundancy of the suspension bridge structure, the damage of a single sling had minimal impact on the overall bridge damage. In this study, a previously cited stress ratio[23] was utilized as the damage index for both the suspender and the main cable to classify the damage. The main cable of LDYB utilized parallel steel wires with a tensile strength of 1 960 MPa. The values of the damage indices of each key component are shown in Table 1.

Table 1 Damage indices of bridge components

Damaged component	Damage index	Minor damage	Medium damage	Severe damage	Complete damage
Tower bottom section	φ/m^{-1}	1.68×10^{-5}	1.85×10^{-4}	2.22×10^{-4}	5.65×10^{-4}
Section of the middle beam	φ/m^{-1}	3.33×10^{-5}	2.59×10^{-4}	3.18×10^{-4}	6.45×10^{-4}
Tower top section	φ/m^{-1}	7.01×10^{-6}	2.10×10^{-4}	3.09×10^{-4}	1.36×10^{-3}
Pier bottom section	φ/m^{-1}	6.84×10^{-5}	6.06×10^{-4}	1.73×10^{-4}	2.19×10^{-3}
Pier top section	φ/m^{-1}	1.69×10^{-5}	5.57×10^{-4}	6.70×10^{-4}	3.06×10^{-3}
Main girder	σ/MPa	275	345	420	
Main cable	σ/σ_y	0.45	0.60	0.75	0.90
Hanger	σ/σ_y	0.75	0.90		

2.4 Damage probability of key components of LDYB

In this study, the response surface method was employed to fit the function in ANSYS software, and the reliability analysis module in ANSYS was used for probability analysis. Considering the uncertainty of structural parameters, the analysis of LDYB accounted for the variability of the elastic modulus and the uncertainty of the cross-sectional area, material density, and bending moment of inertia. By defining input and output variables, the JC method was applied to solve the fitting function at sampling points. Random variable parameters for the structural material of LDYB were selected following Ref. [24] and practical considerations.

2.4.1 Damage probability of key components under wind load

The failure probability of each key component under wind load is shown in Fig. 8. In this figure, H represents the hanger; C represents the main cable; G represents the main girder; T represents the bridge tower; and P represents the bridge pier. Specifically, H1, H2, and H3 correspond to hanger elements Nos. 3, 35, and 40, respectively. C1 and C2 represent main cable elements Nos. 38 and 39, while G1 and G2 correspond to main girder elements Nos. 39 and 103. T1, T2, and T3 denote bridge tower elements Nos. 1, 13, and 27, respectively. P1 and P2 represent bridge pier elements Nos. 1 and 6. The locations of these components are illustrated in Fig. 7. F represents the applied wind force. Specifically, F1 corresponds to the wind speed in the 100-year return period (43.0 m/s). F2 represents the wind speed in the 50-year return period (39.5 m/s). F3 represents the wind speed in the 10-year return period (31.4 m/s).

Among all the components, the main girder at the bridge tower was the most susceptible. It had the highest failure probability for minor damage, indicating that it was the most vulnerable part under wind load. Furthermore, as shown in Fig. 8, the probability of failure increased as the wind load increased for each component. Additionally, the probability of failure decreased as the damage level increased.

2.4.2 Damage probability of key components under seismic load

The failure probability of each component under seismic load is illustrated in Fig. 9. In this figure, E represents the seismic action. E1 denotes the seismic load intensity with a 2% probability of occurrence and a peak seismic acceleration of $0.235g$. E2 represents the seismic

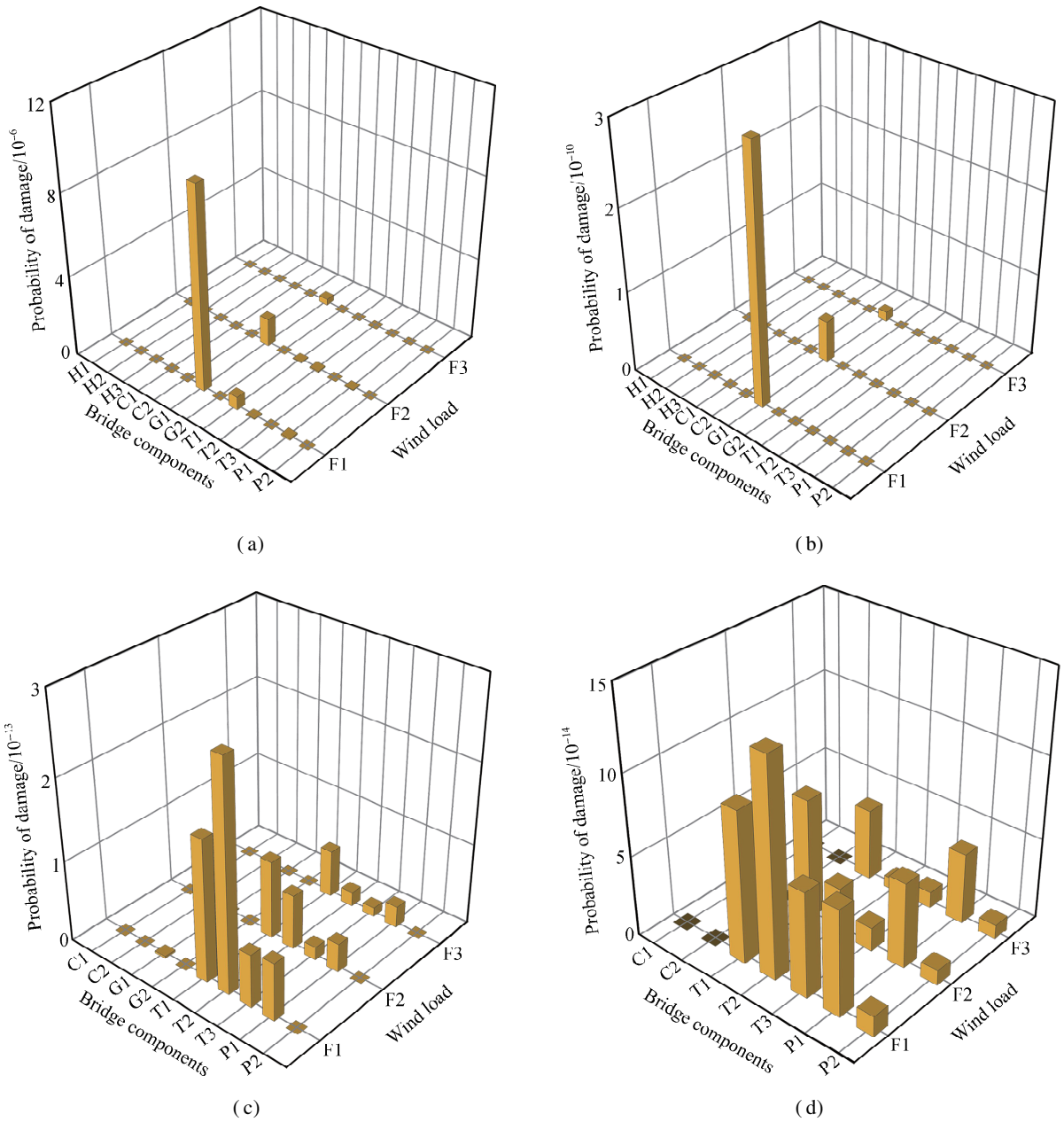

Fig. 8 Failure probability of key bridge components under wind load. (a) Minor damage; (b) Medium damage; (c) Severe damage; (d) Complete damage

intensity with a 5% probability of occurrence and a peak seismic acceleration of 0.179g. E3 indicates the intensity of an earthquake with a 63% probability of occurrence and a peak seismic acceleration of 0.046g.

Under the influence of earthquakes, the failure probability of the bridge tower pier was significantly higher compared with those of the main girder, main cable, and upper structure suspender. This suggests that the safety of the suspension bridge was primarily governed by the substructure when subjected to seismic loads. Similar to wind loads, the probability of minor damage was the highest for each component. As the intensity of the earthquake increased, the failure probability also rose. The higher the damage level, the lower the failure probability.

2.4.3 Damage probability of key components under wind and seismic loads

Under the simultaneous action of wind and seismic loads, the damage probability of the key components of the bridge is shown in Fig. 10. Therein, the impact of earthquakes was more pronounced on the towers and piers, whereas wind predominantly affected the girders, cables, and hangers. When earthquake and wind acted at the same time, the failure probability of the towers and piers exceeded those of the main girder, main cable, and suspension hanger in the superstructure. This implies that during concurrent occurrences of these two disasters, earthquakes have a controlling effect.

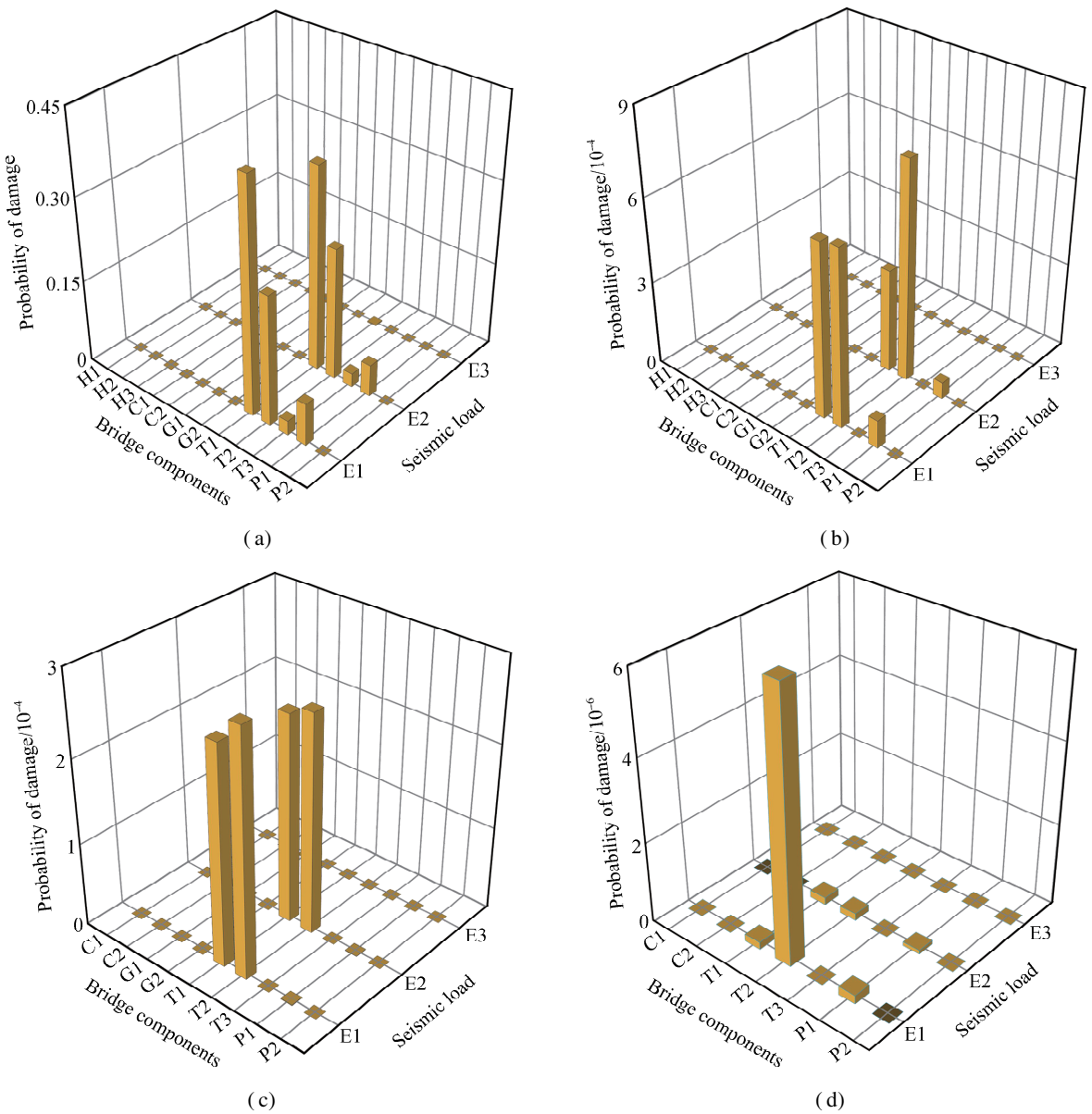

Fig. 9 Failure probability of key bridge components under seismic load. (a) Minor damage; (b) Medium damage; (c) Severe damage; (d) Complete damage

2.5 Development of the improved Bayesian network

After obtaining the damage probabilities of the key components, the improved Bayesian network method was applied to the structural system. In this study, each component of the bridge system was treated as part of a series-mode frame. The Bayesian network model developed in this study is presented in Fig. 11. The key components and the corresponding limited states were numbered accordingly. For example, the hangers consisted of three key components, H1, H2, and H3 with two corresponding damage states: H_{i1} and H_{i2}.

3 Results and Discussion

3.1 Failure probability of LDYB

The failure probability of the entire suspension bridge under different load conditions could be obtained after improved Bayesian network calculation. Apparently, the failure probability of the entire bridge was higher than that of individual components. Therefore, considering the failure risk of only the bridge's individual members is not conservative. Specifically, under wind load, the main girder's damage had the most significant impact on the overall bridge damage. Under seismic load, the tower and pier's damage had the greatest influence on the overall bridge damage.

3.2 Results of LDYB risk assessment

Following the risk assessment criteria, the risk was determined by both the risk consequences and the probability. Under wind load, LDYB was classified as under a level 1 risk, indicating a safe state for the bridge. Even

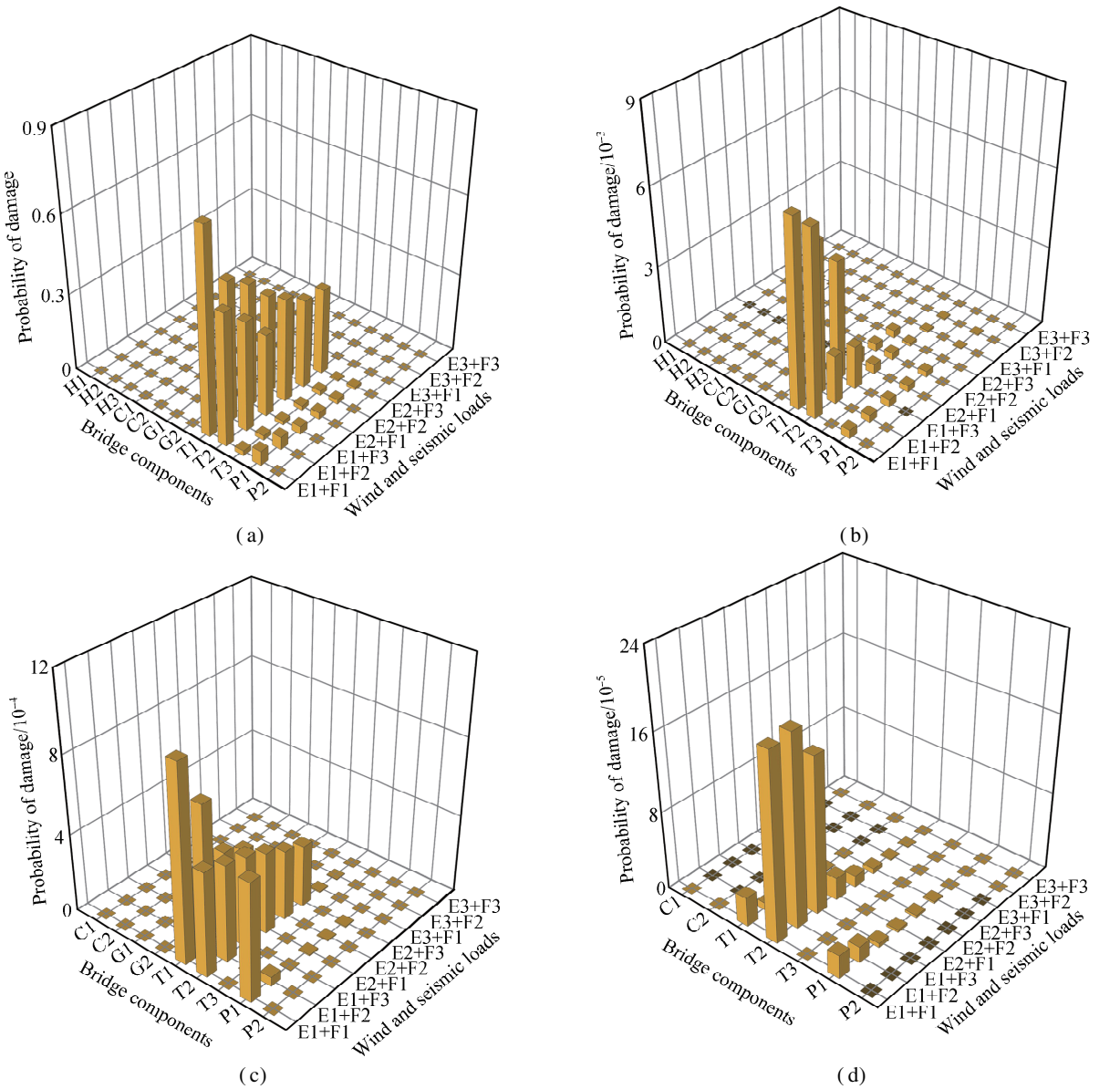

Fig. 10 Failure probability of key bridge components under wind and seismic loads. (a) Minor damage; (b) Medium damage; (c) Severe damage; (d) Complete damage

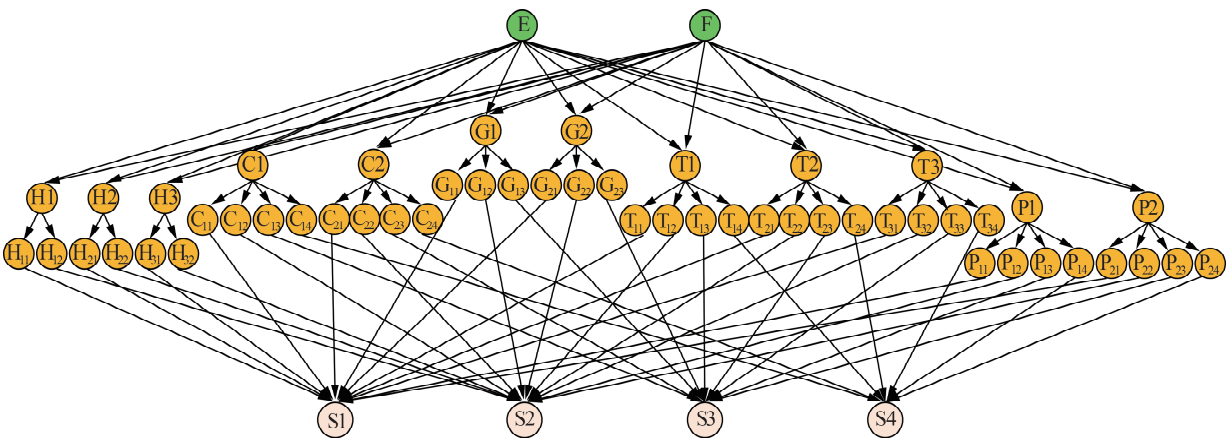

Fig. 11 Improved Bayesian network of reliability of a suspension bridge structure system

under the maximum wind load with a return period of 100 years, the bridge remained in a safe condition. When subjected to an earthquake with a 5% probability of exceedance, the maximum risk level for LDYB was level 3. Furthermore, when wind and seismic loads acted simultaneously, the maximum risk level was also at level 3.

Risk level 3 could be accepted conditionally. Access must be restricted, and emergency plans must be prepared to inspect and repair the cross-sea suspension bridge.

According to the overall design report of LDYB, the bridge was designed for a lifespan of 100 years and followed two levels of seismic fortification standards. Level 1 requires nondamaged cables, hangers, and normal vehicle operation. Level 2 allows slight damage to the towers, main girders, and main cables. For this level, hangers are required to remain undamaged, and the bridge can continue to operate after simple repairs. In accordance with the risk assessment criteria, the risk is determined by both the risk consequences and the probability. For example, when an earthquake with a 4% probability of exceedance occurs, LDYB is classified as under a level 3 risk.

4 Conclusions

1) This study combined the response surface method and JC method to calculate the reliability of whole suspension bridges under seismic and wind loads. A theoretical framework for risk assessment of suspension bridges based on improved Bayesian networks was proposed. The response surface method effectively fitted the performance function under extreme loads, while the JC method handled the nonnormal distribution characteristics of random variables for structural reliability calculations. The integration of these methods enabled efficient reliability analysis of various components, offering a practical tool for assessing the reliability of complex, long-span bridge structures.

2) The improved Bayesian network served as a valuable approach for understanding the relationships between various factors in the risk assessment. It provided clear insights into the interdependencies among network nodes and could be applied to assess the risks associated with complex structural systems, such as suspension bridges. By considering an entire bridge system as a whole and integrating its components, this framework allowed for comprehensive risk analysis of suspension bridges.

3) For LDYB, the analysis results after applying the Bayesian network framework showed that the most serious risk level was level 3. This model could serve as a reference for conducting multihazard risk assessments of sea-crossing suspension bridges.

4) Further research can determine the weights of each component, possibly by using the ratio of strain energy variation before and after structural damage to the strain variable of an intact structure rather than just considering series-mode connections for each component. Moreover, for long-span bridges, other potential hazards, such as flood scouring, could be considered. By incorporating additional disaster types and accumulating more data, the Bayesian network framework can be expanded to provide a more comprehensive assessment of a bridge's life cycle.

References

[1] Ayyub B M. *Risk analysis in engineering and economics* [M]. New York, USA: CRC Press, 2003: 116 − 119.

[2] Yuan Z J, Wang H, Mao J X, et al. Influence of displacement limiting cable on static and dynamic characteristics of three-span continuous suspension bridge [J]. *Journal of Southeast University* (*Natural Science Edition*), 2023, **53**(3): 395 − 401. DOI: 10.3969/j.issn.1001-0505.2023.03.003. (in Chinese)

[3] Liu F. *In-depth investigation and analysis of recent bridge safety accidents*[D]. Changsha: Central South University, 2014. (in Chinese)

[4] Lu G, Wang K, Zhang P. Performance-based system seismic assessment for long-span suspension bridges under two-level seismic hazard[J]. *Journal of Southeast University* (*English Edition*), 2019, **35**(4): 464 − 475. DOI: 10.3969/j.issn.1003-7985.2019.04.009.

[5] Hu J, Guo J, Ou J P. Measurement of wind field characteristics at a long-span suspension bridge[J]. *Journal of Southeast University* (*English Edition*), 2011, **27**(3): 328 − 334. DOI: 10.3969/j.issn.1003-7985.2011.03.020.

[6] Xu W X, Qian Y J, Zhang F, et al. Study on partial safety factors for assessment of existing bridges based on reliability theory considering verification loads[J]. *Journal of Southeast University* (*Natural Science Edition*), 2022, **52**(2): 222 − 228. DOI: 10.3969/j.issn.1001-0505.2022.02.003. (in Chinese)

[7] Su X, Mao J X, Wang H, et al. Automatic identification of modal parameters of long-span bridges considering uncertainty[J]. *Journal of Southeast University* (*Natural Science Edition*), 2023, **53**(5): 850 − 856. DOI: 10.3969/j.issn.1001-0505.2023.05.012. (in Chinese)

[8] Khuri A I, Mukhopadhyay S. Response surface methodology[J]. *WIREs Interdisciplinary Reviews*: *Computational Statistics*, 2010, **2**(2): 128 − 149. DOI: 10.1002/wics.73.

[9] Rackwitz R, Flessler B. Structural reliability under combined random load sequences[J]. *Computers & Structures*, 1978, **9**(5): 489 − 494. DOI: 10.1016/0045-7949(78)90046-9.

[10] Murphy K. Bayes net toolbox for Matlab [EB/OL]. (2001-10-09)[2023-12-20]. https://www.cs.ubc.ca/~murphyk/Papers/bnt.pdf.

[11] Highway Planning and Design Institute. Construction drawing design for the cross-river link between Shenzhen and Zhongshan[R]. Guangzhou: Preliminary Office of Shenzhen-Zhongshan Link Project, 2017. (in Chinese)

[12] Shenzhen-Zhongshan Link Management Center. Investigation report of wind-resistance performance of Lingdingyang Bridge in Shen-Zhong Link[R]. Guangzhou: Preliminary Office of Shenzhen-Zhongshan Link Project, 2018. (in Chinese)

[13] Tao T Y, Gao W J, Jiang Z X, et al. Analysis on wind-induced vibration and its influential factors of long suspenders in the wake of bridge tower[J]. *Journal of Southeast University* (*Natural Science Edition*), 2023, **53**(6): 1065 − 1071. DOI: 10.3969/j.issn.1001-0505.2023.06.

013. (in Chinese)
[14] Spanos P D, Mignolet M P. Simulation of homogeneous two-dimensional random fields: Part Ⅱ—MA and ARMA models[J]. *Journal of Applied Mechanics*, 1992, **59**(2): 275－286. DOI: 10.1115/1.2899499. (in Chinese)
[15] Davenport A G. The spectrum of horizontal gustiness near the ground in high winds[J]. *Quarterly Journal of the Royal Meteorological Society*, 1962, **88**(376): 197－198. DOI: 10.1002/qj.49708837618
[16] Shenzhen-Zhongshan Link Management Center. Bridge location meteorological observation and wind parameter research mid-term report during the feasibility study phase of the Shenzhen-Zhongshan Link Project[R]. Guangzhou: Preliminary Office of Shenzhen-Zhongshan Link Project, 2013. (in Chinese)
[17] Li Y G. Earthquake safety evaluation report of the engineering site of the Shenzhen-Zhongshan Link Project[R]. Guangzhou: Guangdong Engineering Research Institute for Earthquake Prevention, 2011. (in Chinese)
[18] Dai X J, Li K M. Programming of artificial seismic wave based on Matlab[J]. *Sichuan Building Materials*, 2018, **44**(9): 75－76. (in Chinese)
[19] Wang X W. *Failure mode, seismic vulnerability and risk assessment of cable-stayed bridges under earthquake action*[D]. Chengdu: Southwest Jiaotong University, 2017. (in Chinese)
[20] Liang Z Y. *The theory of seismic design of irregular high-pier bridges*[D]. Shanghai: Tongji University, 2007. (in Chinese)
[21] Huang W, Gould P L. 3-D pushover analysis of a collapsed reinforced concrete chimney[J]. *Finite Elements in Analysis and Design*, 2007, **43**(11/12): 879－887. DOI: 10.1016/j.finel.2007.05.005.
[22] Highway Planning and Design Institute. Code for design of highway steel structure bridges: JTG D60—2004 [S]. Beijing: China Planning Press, 2015. (in Chinese)
[23] Cao L. *Research on structural vulnerability of three-tower self-anchored suspension bridge based on reliability theory*[D]. Xi'an: Chang'an University, 2019. (in Chinese)
[24] Imai K, Frangopol D M. System reliability of suspension bridges[J]. *Structural Safety*, 2002, **24**: 219－259. DOI: 10.1016/S0167-4730(02)00027-9.

基于改进贝叶斯网络方法的跨海悬索桥多灾害风险评估

柳成荫[1,2] 任立辰[1,2] 江兆烁[3] 方其样[1,2]

([1]哈尔滨工业大学(深圳)土木与环境工程学院, 深圳 518055)
([2]哈尔滨工业大学(深圳)广东省土木工程智能韧性结构重点实验室, 深圳 518055)
([3]School of Engineering, San Francisco State University, San Francisco 94132, USA)

摘要:为评估大跨度悬索桥在持续风荷载和偶发地震下的综合风险,将桥梁运营期间结构损伤概率的定量分析和损伤后果的定性评估相结合,提出了一种基于改进贝叶斯网络的跨海悬索桥风险评估框架. 首先,分析桥位处的风灾和地震灾害,根据悬索桥的特点获取各构件的损伤程度;其次,利用结构可靠度理论,计算桥梁结构失效概率;最后,提出了基于改进贝叶斯网络的悬索桥风险评估模型,并对桥梁运营期风险进行评估. 结果表明,考虑不同构件对桥梁的影响程度,根据桥梁的承灾能力将桥梁损伤分为 4 级. 以伶仃洋大桥为例,采用所提方法得到多灾害风险下该桥最大风险等级为 3 级,需限制通行并进行检修,说明该方法能够指导跨海桥梁应对多风险灾害的应急管理策略.

关键词:跨海悬索桥;风险评估;贝叶斯网络;致灾因子;结构可靠度
中图分类号:TU448.25